Chip formation and strain localization in 100Cr6

R. Clos, U. Schreppel, P. Veit

Institut für Experimentelle Physik/Otto von Guericke Universität, Magdeburg

Abstract. Chip formation and adiabatic shear banding, which is the basic mechanism for segmented chips, was investigated in 100Cr6 as well as some other steels. Adiabatic shear banding, which is governed by a set of coupled highly nonlinear differential equations, should be one reason for size effects during cutting. Tests were performed using cylindrical, flat hat-shaped and U-shaped cutting specimens, respectively, in a modified Split-Hopkinson-Pressure-Bar set-up. The flat and the cutting specimen allow the in situ measurement of the temperature field by means of a fast infrared detector array simultaneously with the mechanical response of the specimen. Two types of arrays (InSb and InGaAs) were used in the localization and postlocalization phase of shear banding, respectively, where the temperatures lie in different ranges. Special interest is given on the development of the localization process from the early stage up to well-developed bands and/or failure. The summarized result of the observations on shear banding is that "adiabatic shear bands" were formed during the postlocalization phase by friction processes. The process of chip formation depends strongly on the hardness for 100Cr6. In a first stage, a geometry dependent transition from discontinuous to continuous chip formation has been found, which is a sign of the occurrence of size effects.

1 Introduction

Strain localization, which manifests in so-called adiabatic shear bands and/or failure, is the basic process of chip segmentation in many metallic materials [1] especially in cutting of hardened steel [2]. It is widely accepted, that the localization phenomenon itself is connected with a plastic instability due to thermal softening [3] (and other softening mechanisms such as texture development, dynamic recrystallization, damage processes etc.). There are numerous studies, focused on both the mechanics and microstructural aspects of the process [3-7]. In the present study, it is investigated in which stage of the localization process sharp shear bands were formed (e. g. the well known "white" bands, which were found in many steels). Special interest is on the question if they are connected with the plastic instability immediately or if they are the result of other processes. Because strain localization is a highly nonlinear phenomenon size effects should occur at machining, e.g. a transition from continuous to discontinuous chip formation depending on the geometry of the system. These effects may be understood only if the process of strain localization can be described sufficiently [8,9].

2 Experimental methods

The Split-Hopkinson-Bar technique was applied, in generally with pulse duration of 80 µs. The well known cylindrical hat-shaped and "flat hat-shaped" specimens (which were specially designed in order to reduce edge effects) were used in the strain localization experiments [10], respectively. The flat specimen type allows the measurement of the temperature during the strain localization. The set-up is shown in Figure 1.

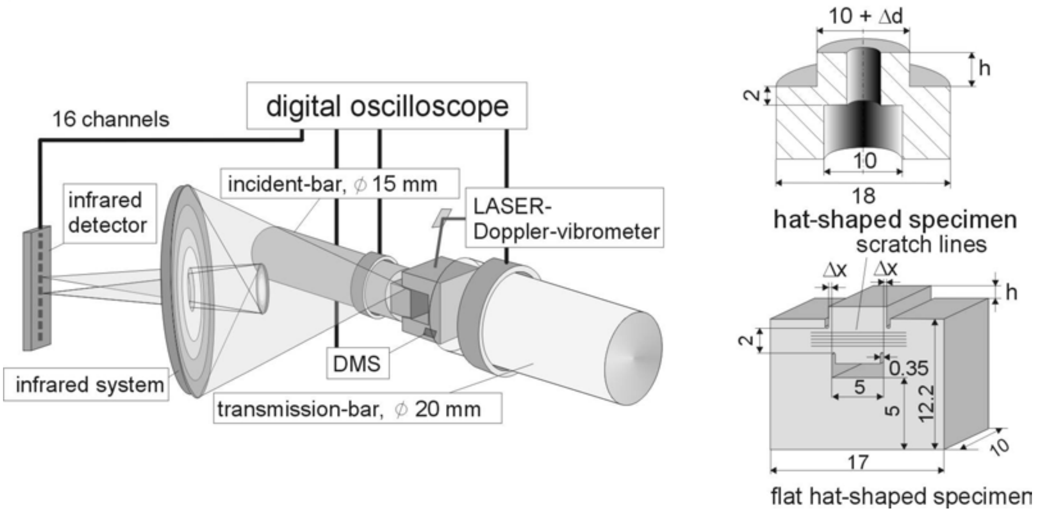

Fig. 1: Experimental set-up/strain localization and geometry of the specimen

Different stages of localization are investigated by changing the height of the hat. The local temperature was determined by measuring the infrared radiation from the surface by means of a fast infrared detector array. The array consists of 16 single elements. Two types of detector materials (InSb and InGaAs) were used. The signals of each detector element were amplified using low noise amplifiers and recorded (16 channels, 12 bit). The whole system is properly calibrated, taking care for similar emissivity of gauge and shear band specimens, respectively. Depending on the detector type, the realized lateral resolution and the necessary time resolution there are lower limits of the detectable temperature, InSb: about 50°C at 10 µm lateral resolution (the upper limit is under the given conditions about 600°C), InGaAs: about 550°C at 5.5 µm. For that reason the InSb-detector is especially suited for the investigation of the quasi-homogeneous deformation and the initial phase of localization, respectively, while the InGaAs-detector is used in the postlocalization phase.

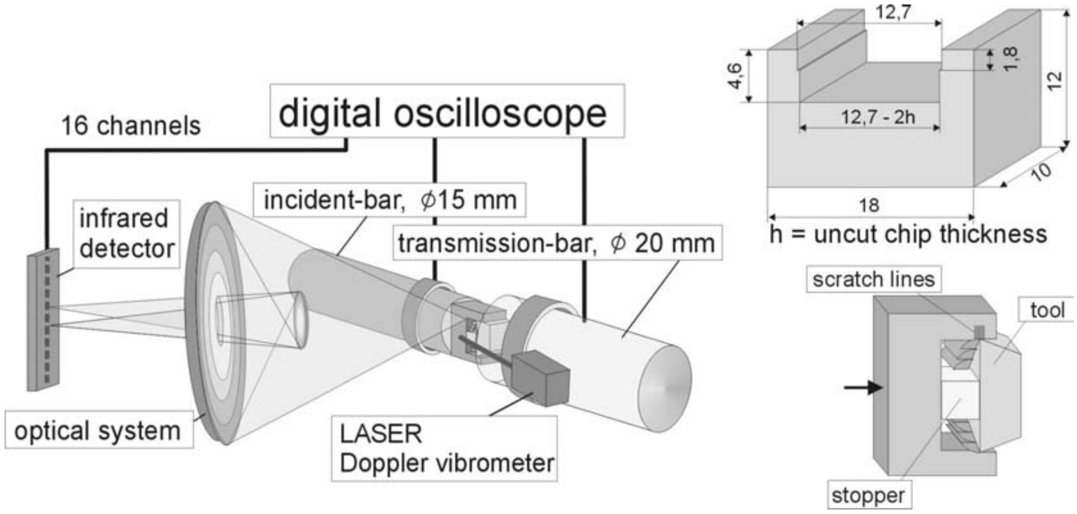

Fig. 2: Experimental set-up/cutting and geometry of the specimen

The set-up for the cutting tests is shown in Fig. 2; there U-shaped specimens are used. The cutting tool rests, while the specimen moves. In this way, measurements of the temperature as well as imaging methods are applicable. 2D-conditions are realized in the cutting process approximately. Fig. 3 shows the set-up, which is used in connection with an ultra high-speed video camera* (* Shimadzu Hyper Vision HEX-108 with ISIS V2 camera chip 10^6 frames/s, 312 x 260 pixels, 100 frames). With the video technique new insight into details of the localization and chip formation process, respectively, is gained.

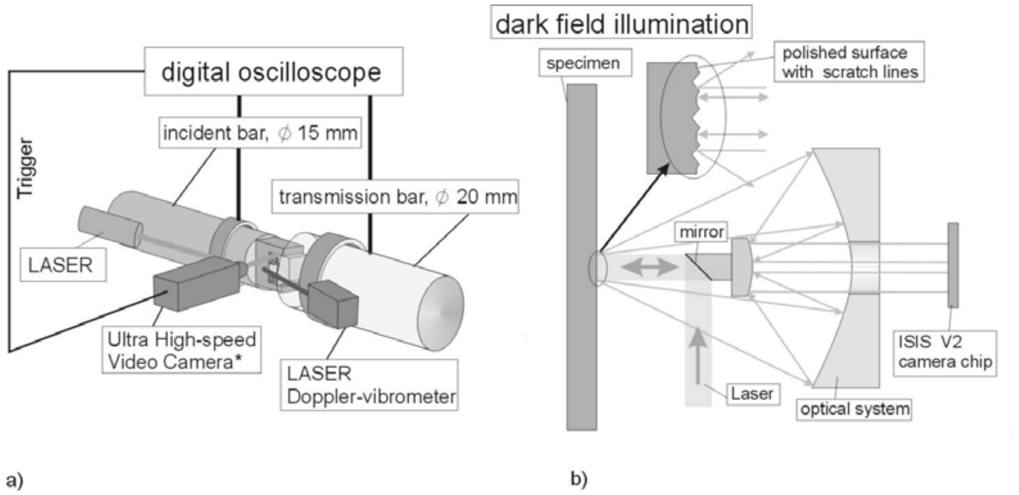

Fig. 3: Experimental set-up/ultra high-speed camera a) and illumination principle b)

The investigated materials were 100Cr6, 50CrV4 and Ck45 (the latter two for comparison) in different states of hardness. The microstructure of the specimens was analysed by means of metallography, scanning and transmission electron microscopy (SEM, TEM).

3 Strain localization

Figure 4 shows the stress σ_T measured in the transmission bar versus the relative displacement Δh of the hat of the specimen (strain gauges, which were applied on the surface of the flat specimens, give nearly the same curves but with reduced oscillations).

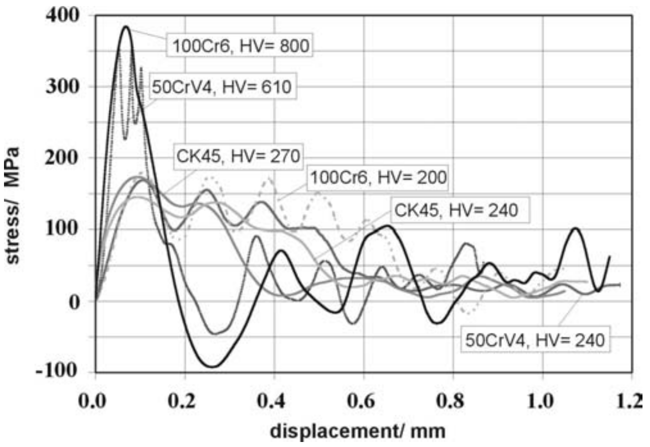

Fig. 4: Development of the transmitted pulses versus "hat" displacement (see also Fig.1) in different materials

Δh increases nearly linear with the time, usually the slope increases slightly at the end of the localization phase, but is then constant again. With exception of 100Cr6 at high hardness (HV > 700) in all cases of Figure 4, narrow "white" bands can be found in the specimens (bandwidth from about 1 µm in 100Cr6 up to about 20 µm in Ck45) at sufficiently long loading duration. Complete failure occurs if the inclination of the ligament is too small or the hardness is too high.

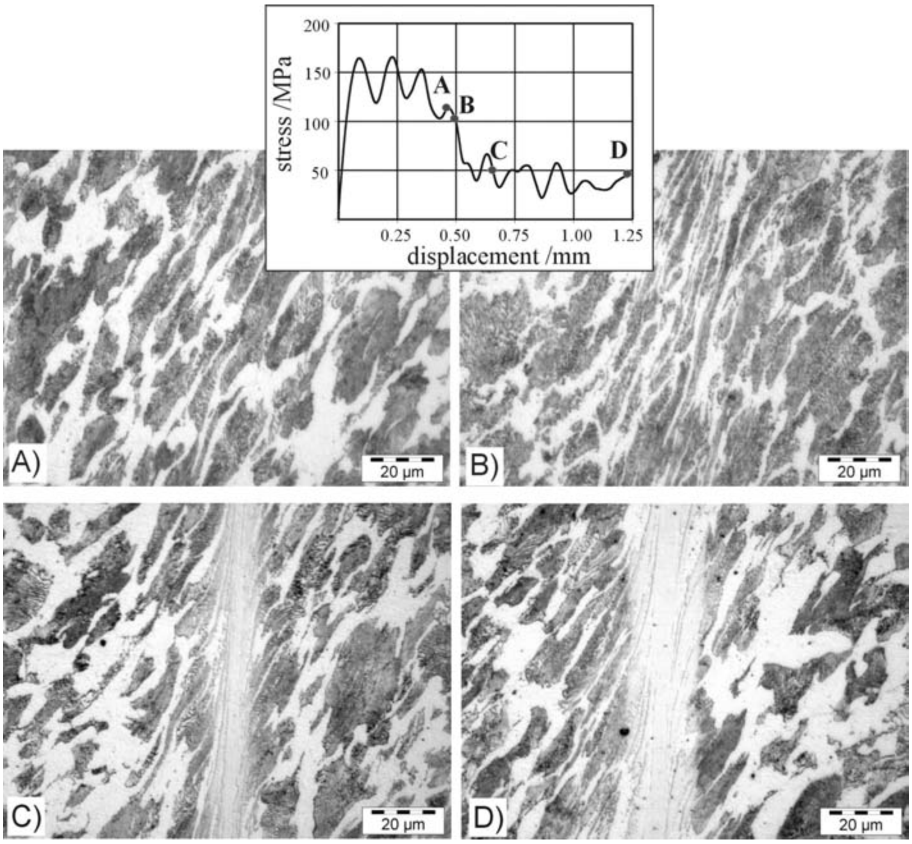

Fig. 5: Evolution of the shear band morphology for pearlitic-ferritic steel Ck45

In other experiments, the loading was stopped at the marked points; the corresponding microstructure is shown in Fig. 5 for Ck45. It is to distinguish between the prelocalization phase (about up to point A), the localization phase (from points A to C) and the postlocalization phase. There is a quasi-homogeneous shear deformation in the prelocalization phase. The width of this region (here denoted as "deformation band") is about 200 µm and obviously determined by the geometry of the specimen. The rest of the specimen deforms essentially elastic (this was examined for some of the materials by in situ measurement of the deformation of lines scratched on the surface of the specimen).

At point A unstable localization occurs, the stress drops drastically and further deformation is confined to a narrowing zone, while the rest of the deformation band mentioned above doesn't deform further. This "frozen in" deformation state may be used, in order to determine a critical local shear strain γ_{crit} at which adiabatic shear banding or failure occurs. The critical shear strain was evaluated to 2.2 for Ck45 and about 0.1 only for 100Cr6 (HV > 700), respectively. On the other hand, γ_{crit} is no materials constant. It depends on the superposed pressure, which is not constant over the ligament. This dependence on the triaxiality is quite important in the cutting process. At the point C shear bands were found in parts of the plane of localization (ligament). In other parts of the ligament, usually separations were observed. Small separated regions were observed in the ligament in the localization phase (i.e. during the drop of the stress) already. With higher resolution (SEM), a high void density is found in these regions.

The postlocalization phase is characterized by a low stress level, which depends on the inclination of the ligament. In the steels Ck45 and 50CrV4, the width of the shear band increases during this phase nearly linear from 4 µm (point C) to about 20 µm (point D). The situation is different in 100Cr6; there the bandwidth doesn't grow and the width is 1...2 µm only for the lower hardness state. An evaluation of the shear strain rate within the band (using a mean value of the band width and the measured velocity of the relative displacement) gives values in the order of 10^6...10^7/s in this phase. In principle, all these stages were found in all materials. However, as in the case of hard 100Cr6 the postlocalization phase may be absent, because complete failure occurs in the localization phase already.

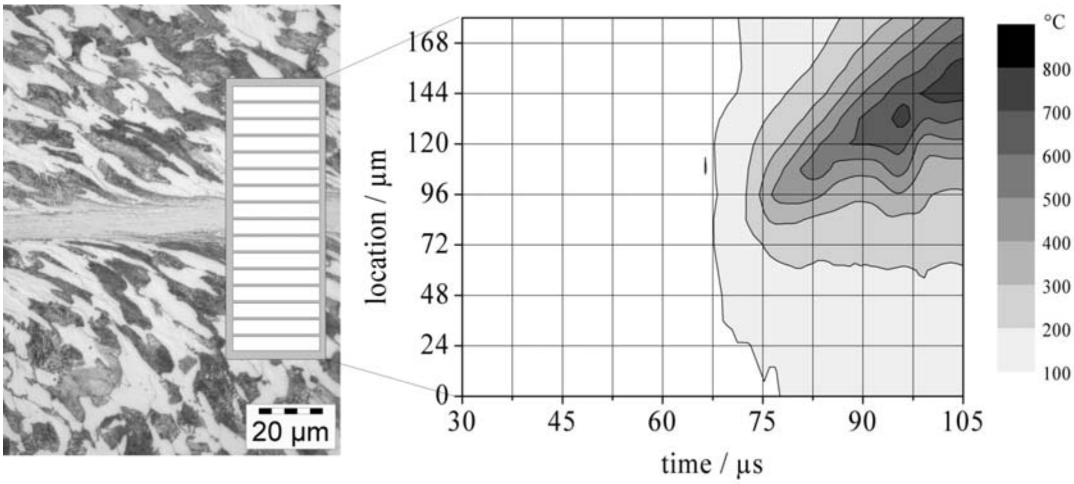

Fig. 6: Temperature distribution for pearlitic-ferritic steel Ck45

Figure 6 shows the measured temperature distributions for the steel Ck45. The detector array is adjusted as shown schematically. The optical system is fixed in space while the specimen moves. So the band is imaged to different detector elements in time if the ligament is inclined to the symmetry plane of the specimen, this explains the right part of Figure 6.

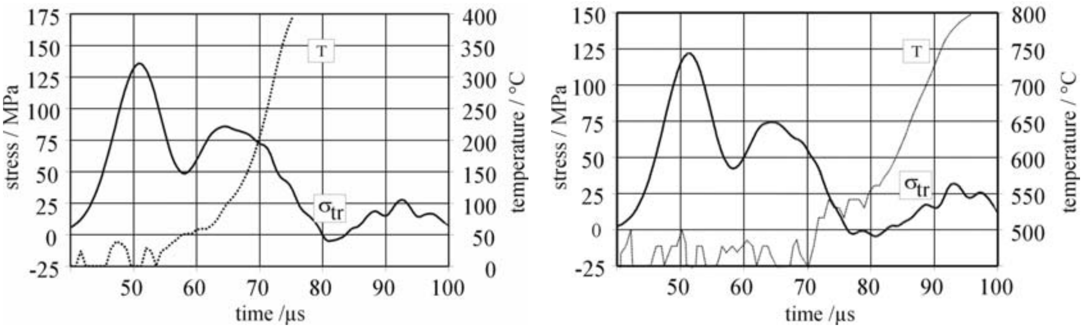

a) b)

Fig. 7: Development of the transmitted pulse and temperature versus time a) InSb infrared detector/77K, b) InGaAs infrared detector

The temperature development is shown in Figure 7 together with the mechanical response (temperatures below 50°C in Figure 7 a and 550°C in Figure 7 b, respectively, are irrelevant due to noise; cf. above). It can be seen, that the localization starts at a temperature of about 200...250°C. The temperature has a value of about 500°C at the beginning of the postlocalization phase and reaches finally about 850°C. The heating rate of the material within the localization zone/shear band is in the order of 10^7 K/s. It can be summarized: a drastic stress drop occurs during localization, while the temperature remains far below the melting temperature, "shear bands" were observed in the postlocalization phase only. The behaviour is similar in 100Cr6 (lower hardness). The main result of numerical simulations of the strain localization is that the stress drop is much slower than in the experiments. Together with the microstructural observation, this indicates that other softening mechanisms especially damage processes have to be included in the material model (also proposed e. g. by Minnaar and Zhou [6]). Somewhat simplified, the localization is terminated by separation of the material along the ligament. The "shear bands" are than products of a completely different process in the postlocalization phase. This has been proved using initially unconnected hat-shaped specimens (Figure 8). The tests were carried out with Ck45.

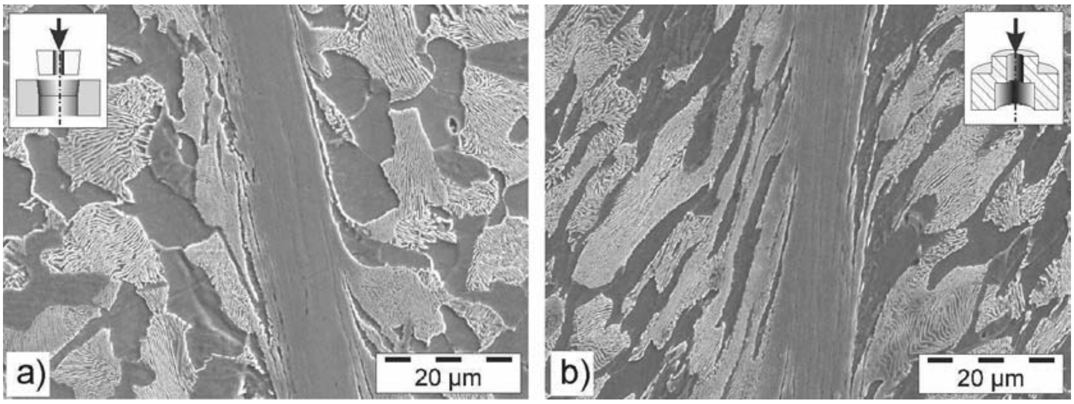

Fig. 8: Band morphology, ferritic-pearlitic steel Ck45, a) friction band $\Delta h = 1.20$ mm, b) shear band, $\Delta h = 1.15$ mm

Fig. 8 a shows a band produced by friction under the same loading conditions as the "shear band" in Fig. 8 b (the same was found for 50CrV4). There are no differences in the SEM-picture. TEM-investigations give quite similar structures in both band too, especially the same powder-like diffraction structure. That means that "adiabatic shear bands" are obviously formed by friction and welding processes and not by dynamic recrystallization as discussed in [10]. This fundamental scenario has been confirmed by the high-speed video camera results completely (also for 100Cr6).

4 Chip formation

First orthogonal cutting experiments were carried on 100Cr6 (Fig. 2). In the experiments different hardness states ($210 < HV_{0.025} < 850$) as well as uncut chip thickness h were used. The cutting speed v_c and the nominal rake angle γ were (4.9 – 22.8) m/s and 0°, respectively. Up to h of 200 µm in the lower hardness 100Cr6, only continuous chip formation was observed (Fig. 9a). This agrees with the cutting behaviour of Ck45 and 50CrV4 at comparable hardness [1]. Nevertheless, a change of the chip formation mechanism could occur at still higher uncut chip thickness.

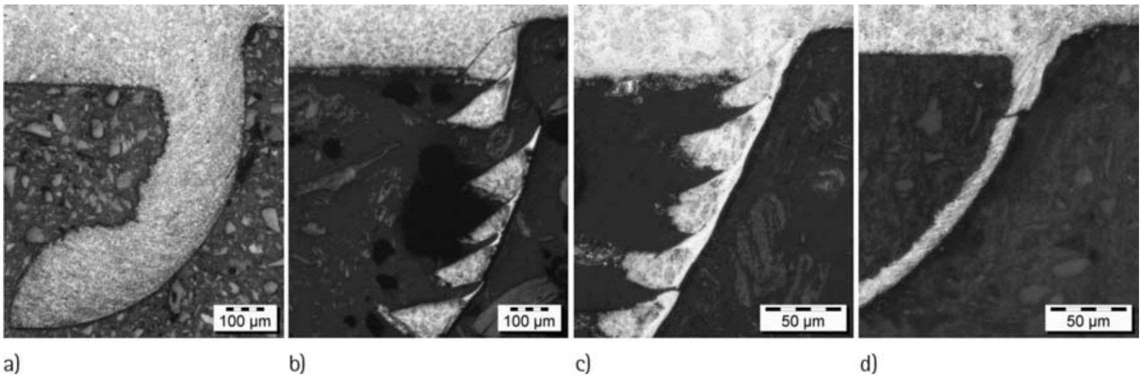

Fig. 9: Chip morphology, cutting condition: a,b) r_β = 60 µm, c,d) HV = 720, r_β = 40 µm
a) HV = 210, v_c = 22.8 m/s, h = 140 µm, b) HV = 810, v_c = 5.3 m/s, h = 130 µm
c) h = 35 µm, v_c = 5.7 m/s, d) h = 20 µm, v_c = 6.0 m/s

100Cr6 with HV > 650 gives segmented chips always at nearly the same uncut chip thickness as above. The chip segments are partially connected by shear bands (Fig. 9b, 9c).

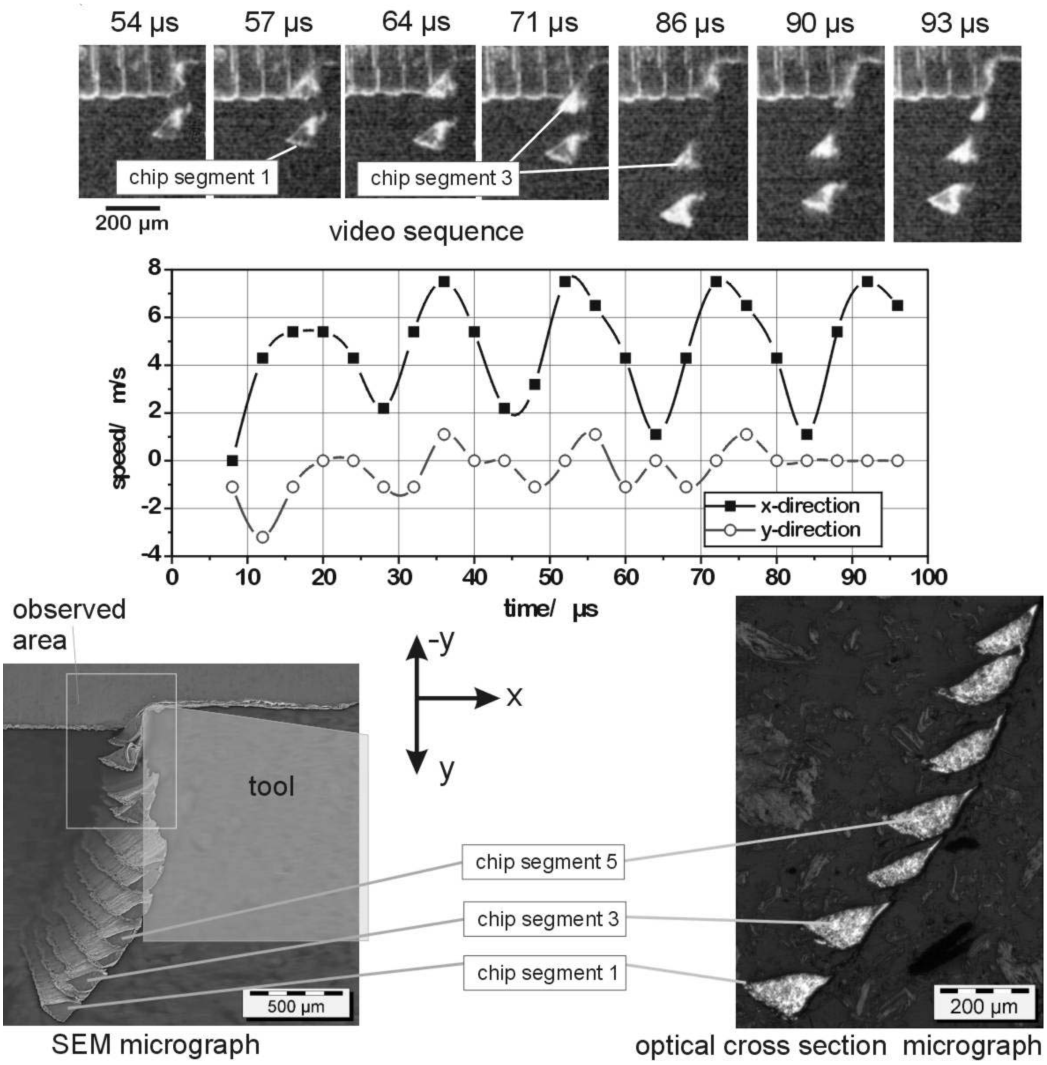

Fig. 10: Orthogonal cutting of the steel 100Cr6/ultra high-speed video (Fig.3), HV = 800, v_c = 4.9 m/s, h = 120 µm, r_β = 60 µm

Investigations of the microstructure show clearly that the frozen-in deformation at the boundary of the bands (cf. above) is much higher than in the strain localization experiments. The reason for is the much higher (negative) triaxiality during cutting. In principle, all stages of segmented chip formation were confirmed, which had been described in [1] for higher strength materials. That is, there is a deformation phase, in which the conditions for strain localization are developed, followed by unstable localization, failure and re-welding.

The high-speed camera images show that the velocity of the specimen oscillates (Fig. 10, it should be reminded that the specimen is pushed against the cutting tool in our experiments). The velocity is low in the deformation phase, while it is high in the localization phase, where the new segment moves away (inserts in Fig. 10). The velocity oscillations correspond with oscillations of the cutting force, which can be calculated from the transmitted pulse σ_{tr}.

If the uncut chip thickness h is reduced to about 20 µm a change of the mechanism has been found really. At this uncut chip thickness also in 100Cr6 (HV = 720) continuous chip formation occurs (Fig. 9d). This geometry dependent transition from discontinuous to continuous chip formation is one of the size effects in hard turning, which has to be explained in future, see also [11]. First analytical investigations of the strain localization phenomenon show that there is e.g. a bifurcation of the propagation behaviour of disturbances in highly nonlinear visco-thermoplastic materials, which might be connected with this transition (will be published elsewhere).

5 References

[1] Clos R., Schreppel, U., Veit, P. in: final report DFG-SPP 1057 "Metal Cutting at High Cutting Speeds", to appear 2004.

[2] Tönshoff H.K., Arendt C., Ben Amor R., Annals of the CIRP **49** (2000) 547-566.

[3] Wright T.W., The Physics and Mathematics of Adiabatic Shear Bands (University Press, Cambridge, 2002).

[4] Batra R.C., Kim C.H., Comp. Mech. **23** (1999) 8-19.

[5] Pérez-Prado M.T., Hines J.A., Vecchio K.S., Acta Mater. **49** (2001) 2905-2917.

[6] Minnaar K., Zhou M., J. Mech. Phys. Solids **46** (1998) 2155-2170.

[7] Xue Q., Meyers M.A., Nesterenko V.F., Acta Mater. **50** (2002) 575-596.

[8] Gao, H., Huang, Y., Scripta Materialia **48**(2003), 113 – 118.

[9] Hughes, D.A., Hansen, N., Bammann, D.J., Scripta Materialia **48** (2003), 147 – 153.

[10] Clos R., Schreppel U., Veit P., J. Phys. IV France **10** (2000) 257-262.

[11] Denkena, B., Becker, J.C., Jivishov, V., Proceedings of the 1st Colloquium Processscaling, Bremen, 28./29.10. 2003.